

# Spectroellipsometric studies of sol-gel derived $\text{Sr}_{0.6}\text{Ba}_{0.4}\text{Nb}_2\text{O}_6$ films

Melanie M. T. Ho and T. B. Tang

*Department of Physics, Hong Kong Baptist University, Kowloon Tong, Kowloon, Hong Kong SAR*

C. L. Mak,<sup>a)</sup> G. K. H. Pang, K. Y. Chan, and K. H. Wong

*Department of Applied Physics, The Hong Kong Polytechnic University, Hung Hom, Kowloon, Hong Kong SAR*

(Received 4 November 2005; accepted 23 July 2006; published online 31 October 2006)

$\text{Sr}_{0.6}\text{Ba}_{0.4}\text{Nb}_2\text{O}_6$  (SBN) films have been fabricated on (001)Si substrates by a sol-gel technique. The annealing process was carried out in air at various temperatures ranging from 200 to 700 °C. Studies using x-ray diffractometry, high resolution transmission electron microscopy, and scanning electron microscopy showed that polycrystalline films, with a grain size of about 100 nm, were obtained only for annealing temperatures  $\geq 600$  °C. The optical properties of these sol-gel derived SBN films were studied by spectroscopic ellipsometry (SE). In the analysis of the measured SE spectra, a triple-layer Lorentz model has been developed and used to deduce the optical properties of the SBN films. Our systematic SE measurements revealed that the refractive indices of the SBN films increase with the annealing temperature. This increase is more pronounced at around the crystallization temperature, i.e., between 500 and 600 °C. The extinction coefficients of the films also exhibit a similar trend, showing a zero value for amorphous films and larger values for films annealed at above 600 °C. Our results demonstrate that while crystallization helps to raise the refractive index of the film due to film densification, it also promotes scattering by grain boundary, resulting in a larger extinction coefficient. © 2006 American Institute of Physics.

[DOI: [10.1063/1.2356916](https://doi.org/10.1063/1.2356916)]

## I. INTRODUCTION

Thin film ferroelectrics offer unique electro-optic characteristics that could improve the performance of many integrated optical devices. Potential applications include waveguide modulators and Bragg deflectors.<sup>1</sup> The most commonly used electro-optic material, lithium niobate ( $\text{LiNbO}_3$ ), has an electro-optic coefficient of  $3.1 \times 10^{-11}$  m/V.<sup>1</sup> In comparison, strontium barium niobate,  $\text{Sr}_x\text{Ba}_{1-x}\text{Nb}_2\text{O}_6$  (SBN,  $0.25 \leq x \leq 0.75$ ), possesses a much larger value of  $1.8 \times 10^{-10}$  m/V.<sup>1</sup> Fabrication and characterization of strontium barium niobate films are therefore of great interest and have been reported.<sup>2-7</sup>

Thin film fabrication techniques based on sol-gel method have the advantages of excellent homogeneity, ease of chemical composition control, high purity, low processing temperature, and uniformity over a large area. For optical thin films, it is beneficial to study the effects of the processing parameters on their optical properties. In this paper, the influences of annealing temperature, the most important processing parameter in the sol-gel method, on crystallization, refractive index ( $n$ ), extinction coefficient ( $k$ ), and surface roughness are investigated.

## II. EXPERIMENT

The precursors used for preparing the SBN sol were strontium alkoxide, barium alkoxide, and niobium alkoxide. These alkoxides were prepared individually by dissolving

strontium metal, barium metal, and niobium chloride, respectively, in 2-methoxyethanol. The individual alkoxides were then mixed together to form the SBN sol according to the desired stoichiometric ratio of Sr/Ba=60/40. The mixed solution was refluxed at 120 °C for about 1 h in order to reach the desired sol concentration of 0.16 M. The sol was spin coated on  $1 \times 1$  cm<sup>2</sup> (001)Si substrates using a spin coater operated at 3000 rpm for 30 s. After drying the as-grown films on a hot plate for several seconds, the films were annealed in air at temperatures between 200 and 700 °C for 2 h. Before the coating process, the Si substrates were dipped into a 10% HF solution for 15 min to remove the native oxide layer. The crystallographic structures of the films were studied by x-ray diffractometry (XRD, Philips X'pert) using  $\text{Cu } K_\alpha$  radiation. Studies of high resolution transmission electron microscopy (HRTEM) were carried out using a JEOL JEM-2011 microscope operated at 200 keV to verify the crystallization of the films. The surface morphology and cross section of the films were examined by field emission scanning electron microscopy (SEM, JEOL 6335F). The thicknesses of the films were determined from the SEM cross-section images. An atomic force microscope (AFM, Burleigh, Metris-2000) was used to determine the lateral grain size and the surface roughness of the films. Throughout the AFM studies, scan areas of  $0.5 \times 0.5$   $\mu\text{m}^2$  operated in contact mode were used. For optical analyses, spectroscopic ellipsometry (SE) measurements were carried out by a variable angle spectroscopic phase-modulated ellipsometer (Jobin Yvon UVISSEL) at photon energy between 1.5 and 3.5 eV with a 0.01 eV interval. An incident angle of 70° was used throughout our SE measurements.

<sup>a)</sup> Author to whom correspondence should be addressed; electronic mail: [paclamak@polyu.edu.hk](mailto:paclamak@polyu.edu.hk)

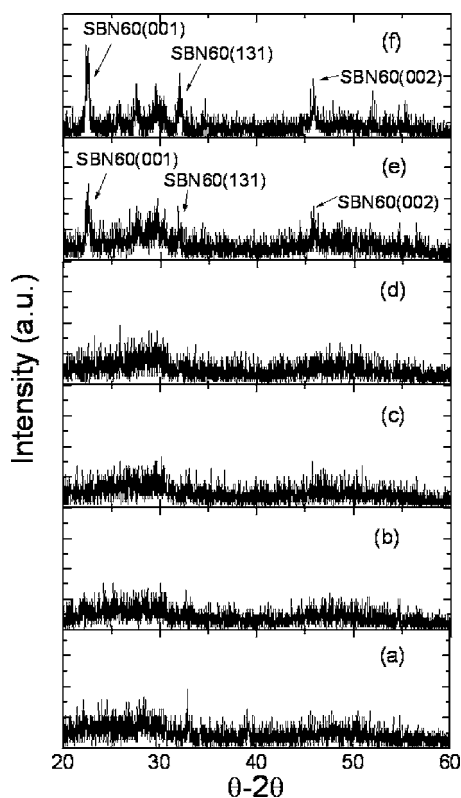


FIG. 1. XRD  $\theta$ - $2\theta$  scans of the SBN films which were grown on Si substrates and annealed at (a) 200 °C, (b) 300 °C, (c) 400 °C, (d) 500 °C, (e) 600 °C, and (f) 700 °C.

### III. RESULTS AND DISCUSSION

XRD  $\theta$ - $2\theta$  profiles of the SBN films annealed at different temperatures are shown in Fig. 1. Due to small thickness ( $\leq 100$  nm), the XRD signals of the films are generally very weak. Regardless of the weak signals, peaks corresponding to the tetragonal-tungsten-bronze (TTB) phase SBN are clearly identified in films with annealing temperatures above 600 °C. As expected, the crystalline films are polycrystalline due to a large lattice mismatch between the SBN film<sup>8</sup> ( $a = b = 12.45$  Å,  $c = 3.94$  Å) and Si substrate ( $a = 5.43$  Å). Due to the poor signal to noise ratio in the XRD measurements, small grains formed at about 600 °C may evade detection. Therefore, high resolution TEM studies were carried out to confirm the occurrence of fully crystallized SBN films annealed at 600 °C.

Figures 2(a) and 2(b) show the HRTEM micrographs of SBN films annealed at 500 and 600 °C, respectively. The cross-sectional HRTEM image in Fig. 2(a) shows amorphous SBN films grown on Si substrate. The image has been processed in such a way that the high frequency part of the power spectrum was removed to improve the visibility of the original image. The amorphous nature of the SBN annealed at 500 °C is clearly supported by the diffused rings of the diffraction pattern shown in the inset of Fig. 2(a). On the other hand, crystalline SBN grains were undoubtedly observed in the sample annealed at 600 °C. Figure 2(b) shows the cross-section bright-field HRTEM image of the specimen annealed at 600 °C. SBN grains of size about 20 nm are readily observed. The selective area diffraction (SAD) pat-

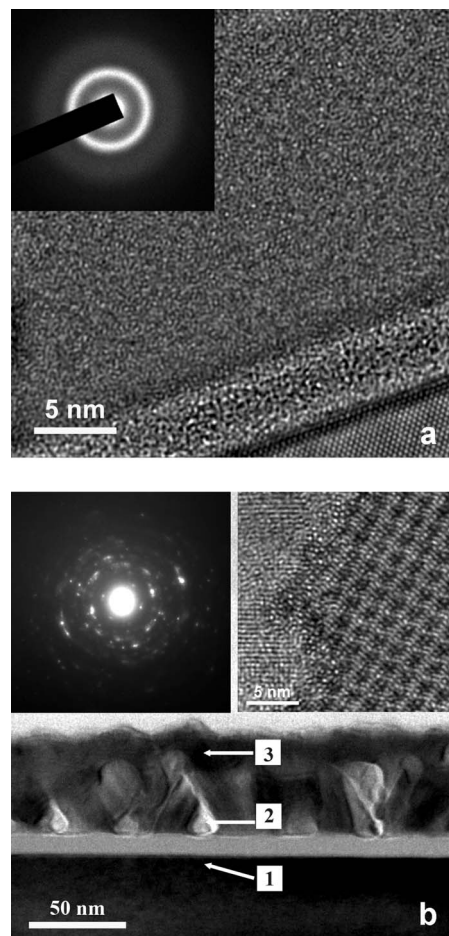


FIG. 2. HRTEM micrographs show the microstructure of SBN film annealed at (a) 500 °C and (b) 600 °C. Cross-sectional bright-field TEM image of the 600 °C annealed specimen showing crystalline SBN grains. The SAD pattern in the top left of (b) shows a growth without preferential direction. The HRTEM image in the top right is obtained from a grain along the 001 direction. Note that there is no amorphous phase in the grain boundaries. In (b), EDS spectra were obtained from three different points which are located across the films.

tern at the top left of Fig. 2(b) shows that there is no preferential direction developed during the growth. High resolution TEM image at the top right is obtained from a grain along the 001 direction. It shows that no amorphous phases are present along the grain boundaries. Most of the grains observed in this specimen show no intergranular amorphous phase. The HRTEM results, together with the XRD results, confirm that the crystallization of our SBN films occurs at about 600 °C.

SEM was employed to examine the surface morphology of these films. All SBN thin film surfaces are, in general, dense, smooth, and crack-free. Figure 3 shows the SEM micrograph of the surface of the SBN film annealed at 600 °C. In the figure, grains with grain sizes of about 100 nm are observed. These grains are elongated, cylindrical in shape, and evenly distributed over the substrate. For films annealed at or below 500 °C (figures not shown), no observable grainy features are detected.

We performed optical studies of these sol-gel derived SBN films by using SE. Generally, SE measures the traditional ellipsometric angles  $\psi$  and  $\Delta$  as a function of energy.

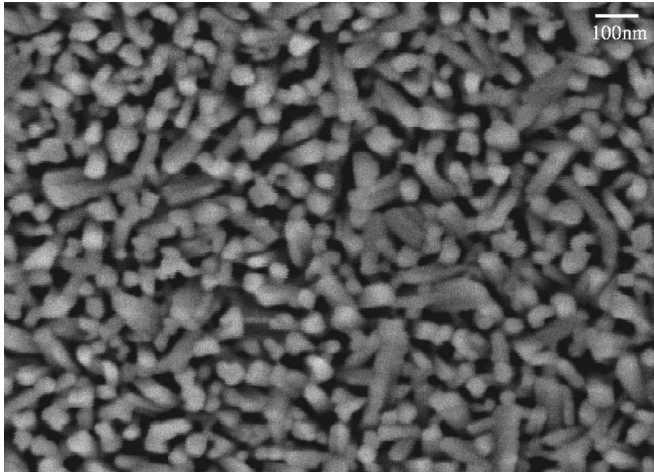


FIG. 3. SEM micrograph of SBN film grown on Si substrate annealed at 600 °C.

However, in our studies, the measured ellipsometric parameters were  $I_S$  and  $I_C$ . The incident light beam was polarized before reflecting from the sample. The reflected beam, after passing through a photoelastic modulator ( $M$ ) and an analyzer ( $A$ ), was dispersed by a monochromator and detected by a photomultiplier tube. The orientations (with respect to the plane of incidence) of the polarizer, modulator, and analyzer are denoted by  $P$ ,  $M$  and  $A$ , respectively. The photoelastic modulator consisted of a fused silica block sandwiched between piezoelectric quartz crystals oscillating at a frequency of  $\sim 50$  kHz. This generated a periodic phase shift  $\delta(t)$  between orthogonal amplitude components of the transmitted beam. The detected intensity in this case would take the general form<sup>9</sup>

$$I(t) = I[I_0 + I_S \sin \delta(t) + I_C \cos \delta(t)], \quad (1)$$

where  $I$  is a constant, and

$$I_0 = 1 - \cos 2\psi \cos 2A + \cos 2(P - M) \cos 2M (\cos 2A - \cos 2\psi) + \sin 2A \cos \Delta \cos 2(P - M) \sin 2\psi \sin 2M,$$

$$I_S = \sin 2(P - M) \sin 2A \sin 2\psi \sin \Delta,$$

$$I_C = \sin 2(P - M) [\sin 2M (\cos 2\psi - \cos 2A) \sin \Delta + \sin 2A \cos 2M \sin 2\psi \cos \Delta]. \quad (2)$$

For a suitable choice of angles  $A$ ,  $M$ , and  $P$ , a simple determination of the ellipsometric angles  $\psi$  and  $\Delta$  from  $I_0$ ,  $I_S$ , and  $I_C$  could be obtained. Throughout the experiment, we set

$$P - M = +45^\circ, \quad M = 0^\circ, \quad \text{and} \quad A = +45^\circ, \quad (3)$$

so that

$$I_0 = 1,$$

$$I_S = \sin 2\psi \sin \Delta, \quad (4)$$

$$I_C = \sin 2\psi \cos \Delta.$$

Therefore, we could calculate  $\psi$  and  $\Delta$  accurately by measuring  $I_S$  and  $I_C$ . Compared with the measurements of  $\psi$  and  $\Delta$  using the null ellipsometry method, the measurements of

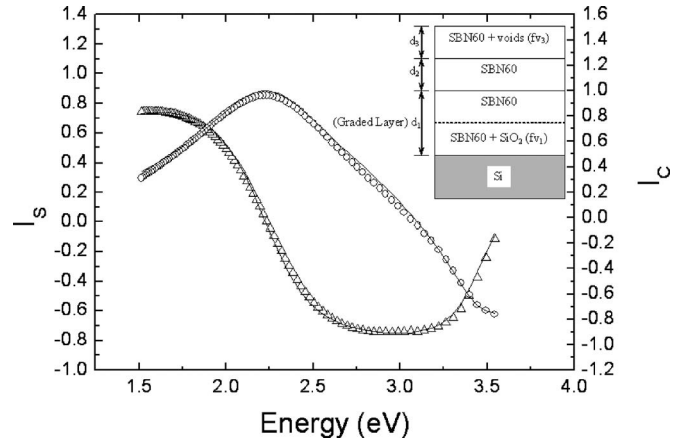


FIG. 4. Spectra of ellipsometric parameters  $I_S$  and  $I_C$  as functions of energy for SBN60 film annealed at 600 °C using the graded triple-layer Lorentz model. The ( $\Delta$ ) and ( $\circ$ ) are the measured  $I_S$  and  $I_C$  values, respectively, while the solid lines are model fitting. Inset of Fig. 4: Graded triple-layer model for interpreting the SBN films.  $fv_1$  and  $fv_3$  are the  $\text{SiO}_2$  and the void volume percentages in the bottom and top layers, respectively.  $d_1$ ,  $d_2$ , and  $d_3$  are the layer thicknesses of the bottom, middle, and top layers, respectively.

$I_S$  and  $I_C$  using the modulation ellipsometry method are much faster.<sup>10</sup>

Figure 4 shows the dispersion curves of  $I_S$  and  $I_C$  as functions of energy for the SBN60 film annealed at 600 °C. In analyzing these profiles, simply the Lorentz model with one oscillator of the dielectric function,

$$\varepsilon(\omega) = \varepsilon_\infty + \frac{f\omega_0^2}{\omega_0^2 - \omega^2 + i\gamma\omega}, \quad (5)$$

is used to describe the energy band gap of SBN. The model parameters  $f\omega_0^2$ ,  $\omega_0$ , and  $\gamma$  are the oscillator strength, resonance energy, and damping rate of the oscillator, respectively. The parameter  $\varepsilon_\infty$  represents the contributions at high frequencies. Initially, a single-layer Lorentz model was used. Here, we assumed that the SBN film was a perfect single layer with a flat surface as well as a smooth and even interface with the Si substrate. A large discrepancy with the experimental data was obtained. In subsequent analysis, we modified the single-layer Lorentz model to a double-layer Lorentz model. In this approach, we assumed that the film consists of dual layers: a bottom bulk SBN layer and a surface layer composed of bulk SBN as well as void. The void in the surface layer was mainly caused by surface roughness and porosity. Indeed, this double-layer model has been very useful in fitting films with rough surfaces. The surface composite layer which comprises both the void and the film materials can describe the surface roughness quite well.<sup>11,12</sup> However, based on this double-layer Lorentz model, poor agreement between the experimental data and fitting results was still obtained. In this two-layer model, we assumed that the SBN film and the Si substrate have a clean and distinct interface. Nevertheless, in this study, the SBN films were fabricated on Si substrates using a sol-gel method. As compared to pulsed laser deposition (PLD) derived films, which require a lower processing temperature and a much shorter annealing time, sol-gel derived films usually have a more severe interdiffusion problem among the substrates and the

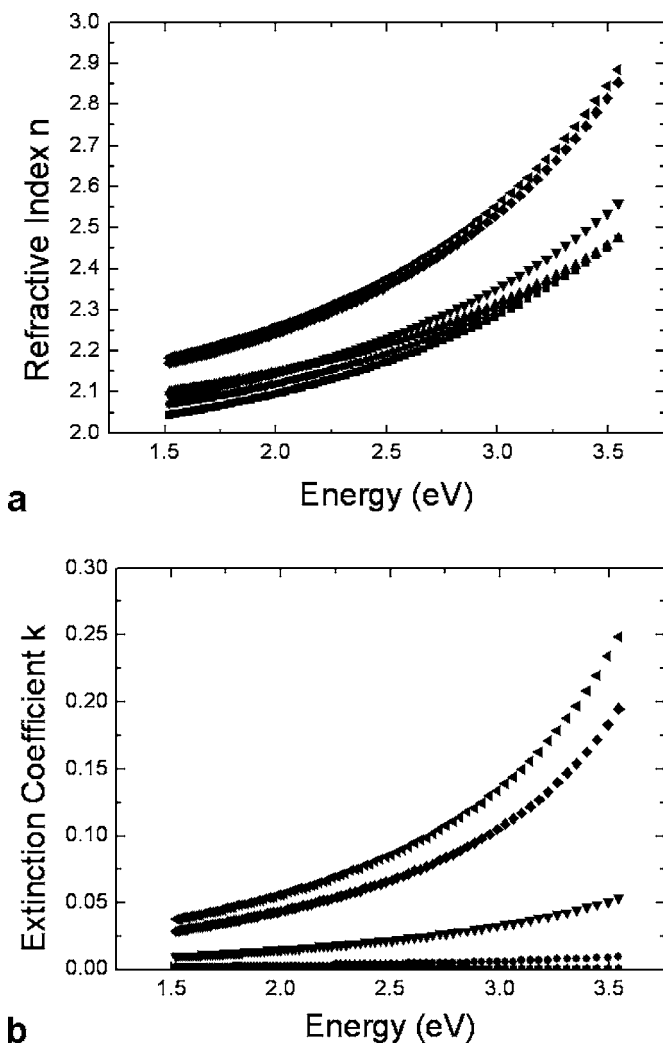


FIG. 5. Dispersion spectra of (a) refractive indices and (b) extinction coefficients of SBN films annealed at 200 °C (■), 300 °C (●), 400 °C (▲), 500 °C (▼), 600 °C (◆), and 700 °C (◄).

films. Therefore, a subsequent modified model based on a graded triple layer (inset of Fig. 4) was used to analyze the data over the spectral range of 1.5–3.5 eV. In this model, the film consists of three layers: a surface layer composed of bulk SBN60 as well as voids, a bulk SBN60 middle layer, and a bottom graded layer linearly mixed with bulk SBN60 and bulk SBN60 plus SiO<sub>2</sub>. Based on this graded triple-layer Lorentz model, we are able to obtain a much better fit with small deviation of  $I_S$  and  $I_C$  for all the samples.

Figures 5(a) and 5(b) show the dispersion spectra of the refractive indices  $n$  and extinction coefficients  $k$  of the SBN films derived from the graded triple-layer model, respectively. In general,  $n$  increases nonlinearly with photon energy over the entire energy range. A more perceptible increase occurs at energies above 2.5 eV. As the annealing temperature increases, the spectra of  $n$  shift upward. The upward shift is more significant at around crystallization temperature of the film, i.e., between 500 and 600 °C. This indicates that the crystallization of the SBN films has an important influence on the refractive index. Furthermore, amorphous films possess a nearly zero extinction coefficient. It means that the films are transparent and neither scattering nor absorption

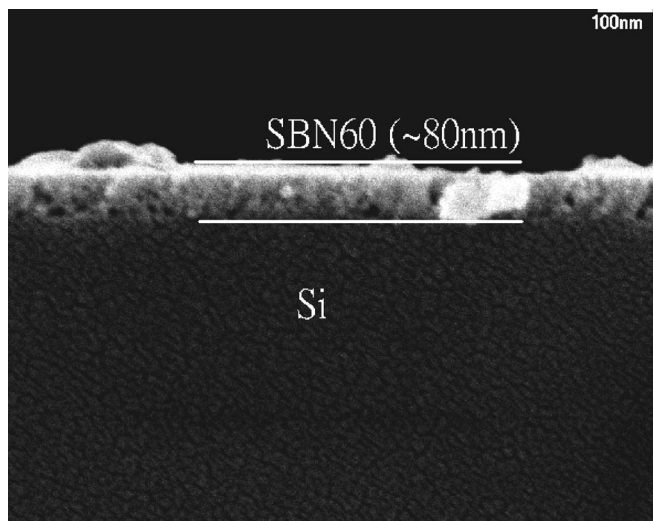


FIG. 6. SEM micrograph showing the cross section of the SBN film grown on Si substrate annealed at 600 °C.

occurs. Meanwhile, for films annealed at 600 and 700 °C, their  $k$  spectra are fairly flat below 2.5 eV and increase more steeply at higher energies. This behavior is typical of an insulator or semiconductor in the range of energy near the band gap. Below the band gap, transmission dominates with a tiny extinction coefficient. As the band gap energy is approached from below, both  $n$  and  $k$  increase with  $k$  advances toward the resonance characterized by the oscillator in the Lorentz model.

Figures 6 and 7 illustrate the cross-section and the surface images of film annealed at 600 °C obtained by SEM and AFM, respectively. The thickness and root mean-square (rms) roughness obtained are about 80 and 7.1 nm, respectively. These values are close to those obtained by SE ( $d_1 + d_2 + d_3 = 75.4$  nm and  $d_3 = 7$  nm). For comparison, the films thickness ( $d_1 + d_2 + d_3$ ) and the surface roughness ( $d_3$ ) obtained by different techniques are listed in Tables I and II. From the tables, we notice that the film thickness and roughness obtained by SE are in good agreement with those obtained by SEM and AFM. These results indicate that the graded triple-layer model is an accurate description for our sol-gel derived SBN films.

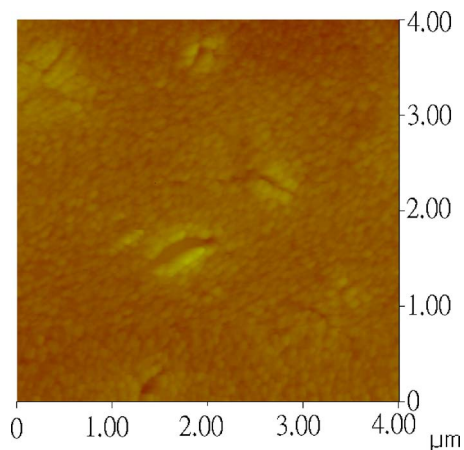


FIG. 7. AFM image of SBN film grown on Si substrate annealed at 600 °C.

TABLE I. Film thickness ( $d_1+d_2+d_3$ ) obtained by different techniques.

Annealing temperature (°C)	SE $d_1+d_2+d_3$ (nm)	SEM $d$ (nm)	% error $\left(1 - \frac{\text{SE } d_1+d_2+d_3}{\text{SEM } d}\right) \times 100\%$
200	99.3	100	0.7
300	91.0	98	7.1
400	83.3	82	1.6
500	80.5	79	1.9
600	75.4	80	5.8
700	85.4	90	5.1

Finally, in order to confirm that the Si substrate has an interdiffusion into our sol-gel derived SBN films, a series of energy dispersive x-ray spectroscopic (EDS) spectra was obtained from points which are located across the interface between the Si substrate and the SBN film annealed at 600 °C as shown in Fig. 2(b). As expected, only Si with no trace of SBN was detected at the substrate (point 1). On the other hand, at the surface of the film (point 3), a reversed result, i.e., only SBN with no traces of Si, was observed. For the interface (point 2), a mixed composition of 25% of Si and 75% SBN was determined. Hence, our EDS data indicate that Si (or SiO<sub>2</sub>) was diffused into the SBN film from the interface. Unfortunately, the spectral resolution of our EDS experiment was about 20 nm, an EDS experiment with a higher spectral resolution (~2 nm) is needed in order to re-

TABLE II. Surface roughness ( $d_3$ ) obtained by different techniques.

Annealing temperature (°C)	SE $d_3$ (nm)	AFM $d_3$ (nm)	% error $\left(1 - \frac{\text{SE } d_3}{\text{AFM } d_3}\right) \times 100\%$
200	8.9	8.3	7.2
300	8.1	7.9	2.5
400	12.3	12.0	2.5
500	7.5	7.9	5.1
600	7.0	7.1	1.4
700	12.0	11.9	0.8

veal the depth profile of our films. Based on our EDS results, we believe that the graded triple-layer model is a reasonable description for our films.

#### IV. CONCLUSION

Sol-gel derived Sr<sub>0.6</sub>Ba<sub>0.4</sub>Nb<sub>2</sub>O<sub>6</sub> (SBN) films fabricated on (001)Si substrates were annealed at different temperatures. SE was used for optical characterization. A graded triple-layer model was developed and used to yield the depth profile, surface roughness, refractive index, and extinction coefficient of these films. It is found that the increase in refractive index is most pronounced at around the crystallization temperature of the films, i.e., 600 °C. The corresponding optical extinction coefficients show a similar trend, suggesting strong scattering loss by grain boundary for crystalline films annealed above 600 °C. The surface roughness and the film thickness obtained from a fitting using the graded triple-layer Lorentz model are consistent with those measured by SEM and AFM.

#### ACKNOWLEDGMENTS

One of the authors (M.M.T.H.) was supported by a Ph.D. studentship of the Hong Kong Baptist University. This research was partially supported by the Research Grant Council of the Hong Kong Special Administrative Region (under Grant No. BQ-556).

<sup>1</sup>Y. Xu, *Ferroelectric Materials and Their Applications* (Elsevier Science, Amsterdam, 1991), p. 83.

<sup>2</sup>Z. Lu, R. S. Feigelson, R. K. Route, R. Hiskes, and S. A. Dicarolis, *Mater. Res. Soc. Symp. Proc.* **335**, 59 (1993).

<sup>3</sup>R. R. Neurgaonkar and E. T. Wu, *Mater. Res. Bull.* **22**, 1095 (1987).

<sup>4</sup>R. R. Neurgaonkar, I. S. Santha, and J. R. Oliver, *Mater. Res. Bull.* **26**, 983 (1991).

<sup>5</sup>S. S. Thony, K. E. Youden, J. S. Harris, Jr., and L. Hesselink, *Appl. Phys. Lett.* **65**, 2018 (1994).

<sup>6</sup>Y. Xu, C. J. Chen, R. Xu, and J. D. Mackenzie, *Phys. Rev. B* **44**, 35 (1991).

<sup>7</sup>C. H. Luk, C. L. Mak, and K. H. Wong, *Thin Solid Films* **298**, 61 (1997).

<sup>8</sup>M. H. Francombe, *Acta Crystallogr.* **13**, 131 (1960).

<sup>9</sup>S. N. Jaspersion and S. E. Schnatterly, *Rev. Sci. Instrum.* **40**, 761 (1969).

<sup>10</sup>H. G. Tompkins and W. A. McGahan, *Spectroscopic Ellipsometry and Reflectometry: A User's Guide* (Wiley, New York, 1999).

<sup>11</sup>K. Y. Chan, W. S. Tsang, C. L. Mak, and K. H. Wong, *Phys. Rev. B* **69**, 144111 (2004).

<sup>12</sup>K. M. Yeung, W. S. Tsang, C. L. Mak, and K. H. Wong, *J. Appl. Phys.* **92**, 3636 (2002).